Chapter 2

# Ti$_2$ZrO Phases Formed in the Titanium and Zirconia Interface after Reaction at 1550°C

2.1 Introduction

Titanium alloys have excellent properties such as high specific strength and corrosion resistance. However, they are very active and tend to dissolve some interstitial elements (e.g. C, N, O, H) of ceramic molds during casting. Saha and Jacob[1] displayed there was an oxidation-reduction reaction between titanium alloys and various oxide molds, and thus, the so-called α-case was formed at the surface of titanium casting, resulting in a hardening and brittle structure.[2-6] That is to say, the oxygen was readily dissolved into the titanium to form α-Ti at the surface of titanium alloys and caused the deterioration of mechanical properties.
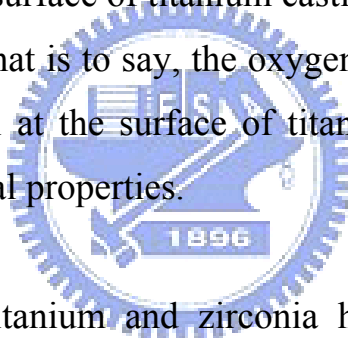
The reactions between titanium and zirconia have been subjected to an intensive investigation, indicating zirconia became oxygen-deficient due to the interfacial reaction. Economos and Kingery[7] revealed that titanium penetrated along the grain boundaries of ZrO$_2$ with the formation of the oxygen-deficient zirconia. Ruh[8] reported that up to 4 at% of titanium were retained in zirconia at room temperature, while up to approximately 10 mol% zirconia would be dissolved in titanium. Zirconium entered into the titanium lattice substitutionally and oxygen entering interstitial positions, but no evidence of other compounds except oxygen-deficient zirconia at the interface was provided.

Some researchers have studied the existence of interfacial phases and the

effects of titanium on the stabilization and mechanical properties of zirconia. Weber *et al.*[9] indicated that zirconia with Ti exceeding the solubility limit showed good strength and thermal shock resistance.   Lin *et al.*[10] stated that zirconia was stabilized due to the dissolution of TiO, formed by the reaction between titanium and residual trace oxygen in the vacuum furnace.   The improvement in the strength and the thermal shock resistance of zirconia was attributed to the dissolution of TiO as well.   According to the pseudobinary diagram of Ti-ZrO_2 proposed by Domagala *et al.*,[11] (Ti, Zr)$_3$O could precipitate from the supersaturated solid solution of α-Ti(Zr, O) during cooling.   However, Weber *et al.*[9] and Lin *et al.*[10] found neither (Ti, Zr)$_3$O nor α-Ti (Zr, O).

Recently, Lin and Lin[12] reported that the interfacial reactions between zirconia and titanium melt resulted in titanium oxides such as Ti_3O or TiO_2 after reaction at 1750°C/7min.   Meanwhile, the lamellae of Ti_2ZrO and α-Ti(Zr, O) were also found.   In present study, the titanium and zirconia diffusion couple was annealed at 1550°C/30min.   The interfacial microstructures were characterized by TEM/EDS.[13]   The orientation relations between α-Ti and Ti_2ZrO were determined using stereographic projection analyses.

2.2   Experimental Procedures

Bulk zirconia specimens used in this study were prepared from the powder of 3mol% Y_2O_3 partially stabilized zirconia (Toyo Soda Mfg. Co., Tokyo, Japan) by hot-pressing in a graphite furnace in vacuum (Model HP50-MTG-7010, Thermal Techno, Inc., California, USA).   The specimens were heated to and held at 300°C for 3 min under 5 MPa with a heating rate of 30°C/min, while heating to and being held at 1450°Cfor 30

min under 30 MPa with a heating rate of 25°C/min. During cooling, pressure was released at 1100°C. The as-hot pressed samples were annealed at 1200°C/4hr so that the stoichiometric ZrO_2 samples were obtained. In the other way, billets of commercially pure titanium (Cp-Ti) were used in this study. Nominal compositions of the starting materials, i.e., zirconia powder and titanium billets, were listed in Table 2.1.

Both zirconia and titanium specimens were cut and machined to the dimensions of 14 mm x 14 mm x 5 mm. Their surfaces were ground and polished to 0.5 μm with a diamond paste, and then ultrasonically cleaned in acetone. One titanium specimen was inserted in between two ZrO_2 specimens to produce a sandwiched sample, and then put in the graphite furnace mentioned above, preparatorily pressed under 5 MPa, evacuated to $2x10^{-4}$ torr, and filled with argon to one atmospheric pressure. This cycle of evacuation and purging was repeated for at least three times. The temperature was raised to 1000°C at the raising rate of 30°C/min, to 1550°C at 25°C/min, and then held at 1550°C for 30 minutes. Thereafter, the temperature was lowered to 1000°C at the cooling rate of 25°C/min, and then furnace cooled down to room temperature.

The microstructures at the interface between zirconia and titanium were characterized using an analytical transmission electron microscope (Model JEM 2000FX, JEOL Ltd., Tokyo, Japan). Cross-sectional TEM specimens perpendicular to the interface of zirconia and titanium were cut into about 3 mm x 2 mm x 0.5 mm. They were ground, polished, and dimpled to 50 μm in thickness. The TEM specimens were then ion milled by a precision ion miller (Model 691, Gatan Inc., California, USA). The quantitative composition analyses were carried out based on the principle of the Cliff-Lorimer standardless technique[13] by an energy dispersive spectrometer

(EDS; Mode ISIS300, Oxford Instrument Inc., London, UK) attached to the TEM.

2.3 Results and Discussion

The lamellae of Ti_2ZrO and α-Ti as well as the orthorhombic β'-Ti were found to exist in the titanium side after cooling down to room temperature, as shown in Fig. 2.1(a). Figure 2.1(b) is a magnified micrograph of the inset area in Fig. 2.1(a), showing the elongated β'-Ti in the middle of the bright field image and Ti_2ZrO lamellae precipitated in the α-Ti matrix. The spherical ordered Ti_2ZrO phase, showing high strain-field contrast due to the lattice distortion, precipitated in α-Ti matrix in the right lower corner (arrowed). It believes that the ordering of Zr and O in α-Ti causes the lattice strain owing to the lattice misfit.

Figures 2.2(a) and (b) display the SADP's of β'-Ti with zone axes of [110] and [111], respectively, being identified as orthorhombic with lattice parameters a= 0.585 nm, b= 0.847 nm and c= 0.606 nm. The EDS in Fig. 2.2(c) indicated that β'-Ti(Zr, O) contained 57.9 at% Ti, 30.7 at% Zr and 11.4 at% O. From the $Ti-ZrO_2$ phase diagram,[11] it is known that hexagonal α-Ti and body-centered cubic β-Ti coexist in Cp-Ti at 1550°C, and the β-Ti will transform into α-Ti during cooling. Oxygen raises the transformation temperature of $\alpha \rightarrow \beta$,[14] causing the α-phase to be stabilized. In despite of the dissolution of a large amount of zirconium, which is a β-stabilizer, β-Ti did not survive but rather transformed to orthorhombic β'-Ti(Zr, O) solid solution during cooling. The transformation of β-Ti to β'-Ti has been investigated in Ti-Al-Nb systems.[15] However, the formation of β'-Ti in the titanium and zirconia system was first found in this study.
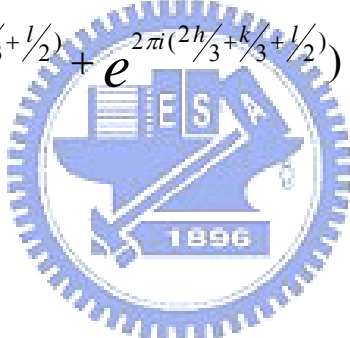
At high temperatures, α-Ti dissolves a large amount of zirconium and oxygen, forming metastably supersaturated disordered solid solution α-Ti(Zr, O), and thus resulting in the precipitation of the lamellae Ti_2ZrO during cooling.   The interlacing lamellar phases were identified as orthorhombic Ti_2ZrO and hexagonal disordered α-Ti from the superimposed SADP's of these two phases shown in Fig 2.3(a).   The streaking of pattern is due to the lamellar shaped effect.   The orientation relations were identified as $[0001]_{\alpha\text{-Ti}}$ // $[110]_{Ti2ZrO}$ and $(10\bar{1}0)_{\alpha\text{-Ti}}$ // $(1\bar{1}0)_{Ti2ZrO}$.   Moreover, the lattice constants of Ti_2ZrO orthorhombic unit cell were calculated as follows: a_o= 0.494 nm, b_o= 0.817 nm and c_o= 0.309 nm, and those of α-Ti hexagonal unit cell are a_h= b_h= 0.301 nm, c_h= 0.468 nm.   Figure 2.3(b) shows the EDS spectrum of the α-Ti, revealing that it comprises 80.7 at% Ti, 8.5 at % Zr, and 10.8 at% O.   Figure 2.3(c) shows the EDS spectrum of the lamellar Ti_2ZrO, consisting of 56.1 at% Ti, 22.9 at% Zr, and 21.0 at% O.   Figure 2.3(d) displays the standard stereographic projection corresponding to Fig. 2.3(a) with $[0001]_{\alpha\text{-Ti}}$ // $[110]_{Ti2ZrO}$.   It indicates that the $(10\bar{1}0)$ plane of α-Ti is parallel to the $(1\bar{1}0)$ plane of Ti_2ZrO in agreement with the result presented by Lin and Lin.[12]

The crystallographic relation between α-Ti (solid line) and the lamellar Ti_2ZrO (dash line) inferred from Fig. 2.3(a) is schematically shown in Fig. 2.4.   The habit planes of Ti_2ZrO and α-Ti are $(10\bar{1}0)_{\alpha\text{-Ti}}$ and $(1\bar{1}0)_{Ti2ZrO}$, respectively.   The stacking sequence of α-Ti is ABABAB.   It reveals that the crystal structure of the orthorhombic Ti_2ZrO is based on that of hexagonal α-Ti with a stacking sequence of ABACABAC.

Figure 2.5(a) shows the superimposed SADP of the spherical ordered Ti_2ZrO phase and α-Ti matrix with $[0001]_{\alpha\text{-Ti}}$ // $[0001]_{Ti2ZrO}$ and $(10\bar{1}0)_{\alpha\text{-Ti}}$ //

$(30\bar{3}0)_{Ti2ZrO}$.   From superimposed diffraction patterns, the spherical ordered phase was identified as hexagonal Ti$_2$ZrO in agreement with the result presented by Fykin et $al.$[17]   The crystal structure of the hexagonal Ti$_2$ZrO was proposed as shown in Fig. 2.5(b).   It indicated that the hexagonal Ti$_2$ZrO unit cell with space group $D_{6h}{}^1$-P6/mmm had one Zr atom at 0, 0, 0 and two Ti atoms at 1/3, 2/3, 1/2 and 2/3, 1/3, 1/2.   Additionally, one O atom was statistically positioned at 1/2, 0, 0; 0, 1/2, 0; 1/2, 1/2, 0.

In order to understand the reflection planes of Ti$_2$ZrO structure, the structure factor of Ti$_2$ZrO would be calculated.   From the atom positions data of Ti$_2$ZrO by Fykin et $al.$[17], the structure factor was calculated as follows:

$$F = f_{zr} + f_{Ti}(e^{2\pi i(h/3 + 2k/3 + l/2)} + e^{2\pi i(2h/3 + k/3 + l/2)}) + f_o(e^{2\pi i(h/2)} + e^{2\pi i(k/2)} + e^{2\pi i(j/2 + k/2)}$$

Multiplication by the complex conjugate , however, would give the square of the absolute value of the resultant wave amplitude $\bm{F}$.

$$|F|^2 = [f_{zr} + f_{Ti}\cos 2\pi(\frac{h+2k}{3} + l/2) + f_{Ti}\cos 2\pi(\frac{2h+k}{3} + l/2) + f_o\cos 2\pi(h/2)$$
$$+ f_o\cos 2\pi(k/2) + f_o\cos 2\pi(h+k/2)]^2 + [f_{Ti}\sin 2\pi(\frac{h+2k}{3} + l/2) +$$
$$f_{Ti}\sin 2\pi(\frac{2h+k}{3} + l/2) + f_o\sin 2\pi(h/2) + f_o\sin 2\pi(k/2) + f_o\sin 2\pi(h+k/2)]^2$$

When all possible values of $\bm{h}$, $\bm{k}$, $\bm{l}$ were considered, the results might be summarized in Table 2.2.   The relative intensities of the diffraction spots in

Fig. 2.5(a) were consistent with the results of calculated Ti$_2$ZrO structure factors. The structure factors of the reflections $(4\bar{2}\bar{2}0)$ and $(2\bar{1}\bar{1}0)$ were $|F|^2 = [f_{zr} + 2f_{Ti} + 3f_o]^2$ and $|F|^2 = [f_{zr} + 2f_{Ti}(1) - f_o]^2$, respectively. The reflection spot of the $(4\bar{2}\bar{2}0)$ plane was thus brighter than that of the $(2\bar{1}\bar{1}0)$ plane as shown in Fig. 2.5(a). Furthermore, the reflection spot of the $(30\bar{3}0)$ plane with $|F|^2 = [f_{zr} + 2f_{Ti}(1) - f_o]^2$ was visible. The $(20\bar{2}0)$ and $(10\bar{1}0)$ reflections were absent, since its structure factor $|F|^2 = [f_{zr} - f_{Ti} - f_o]^2$ were comparatively small and negligible.

The lattice constants of hexagonal Ti$_2$ZrO unit cell were calculated as follows: a=b= 0.902 nm, c= 0.455 nm, and those of α-Ti hexagonal unit cell are a= b= 0.301 nm, c= 0.468 nm. Figure 2.5(c) displays the EDS of spherical ordered Ti$_2$ZrO consisting of 54.2 at% Ti, 22.7 at% Zr, and 23.1 at% O. Figure 2.5(d) shows the standard stereographic projection of the spherical ordered Ti$_2$ZrO and α-Ti corresponding with Fig. 2.5(a), showing the $(10\bar{1}0)$ plane of α-Ti is parallel to the $(30\bar{3}0)$ plane of the spherical ordered Ti$_2$ZrO.

Zirconia was highly soluble in titanium,[11] allowing the formation of a disordered solid solution of α-Ti(Zr, O) at high temperatures. The lamellar and spherical Ti$_2$ZrO phases with different crystal structures were precipitated from the supersaturated α-Ti(Zr, O) during cooling. In contrast, Lin and Lin[12] reported only one of the Ti$_2$ZrO phases in their previous study. According to the Ti-ZrO$_2$ phase diagram,[11] the solubility of ZrO$_2$ in titanium could exceed 20 at%. In the present study, α-Ti dissolved a large amount of Zr and O at 1550℃ forming a supersaturated solid solution α-Ti(Zr, O), whereby Ti$_2$ZrO precipitated. However, a wide two-phase region (23

wt%-75 wt% ZrO_2) of α-Ti(Zr, O) and (Ti,Zr)$_3$O in the Ti-ZrO_2 phase diagram is inconsistent with the coexistence of α-Ti(Zr, O), Ti_2ZrO and β'-Ti in this study.

Lin and Lin reported[12] that the reaction at 1750°C/7min between zirconia and titanium melt caused the formation of the lamellae Ti_2ZrO and α-Ti (Zr, O). However, whether Ti_2ZrO was formed during solidification or by precipitation from α-Ti (Zr, O) during cooling could not be confirmed. Since no liquid α-Ti (Zr, O) existed in this study, it is concluded that the lamellae Ti_2ZrO phase was not formed in the Ti melt but rather precipitated from α-Ti (Zr, O). Furthermore, Lin's report[12] did not find the spherical ordered Ti_2ZrO phase and the β'-Ti in the interface of zirconia and titanium reaction.

2.4   Conclusions

1. In the zirconia/titanium diffusion couple annealed at 1550°C/30 min, titanium was readily to dissolve a large amount of zirconium and oxygen, resulting in metastably supersaturated solid solution.

2. The lamellar and the spherical Ti_2ZrO phases were precipitated from the supersaturated α-Ti solid solution, while the β-Ti coexisting with α-Ti at high temperatures was transformed to the orthorhombic β'-Ti during cooling.

3. The lamellar Ti_2ZrO had an orthorhombic crystal structure with the (110) planes being stacked in the ABACABAC sequence. In the other way, the spherical Ti_2ZrO had a hexagonal crystal structure with Zr and O orderly occupying substitutional and interstitial sites, respectively.

4. The orientation relations between α-Ti and the lamellae orthorhombic Ti_2ZrO were determined to be $[0001]_{α-Ti}$ // $[110]_{Ti2ZrO}$ and $(10\bar{1}0)_{α-Ti}$ //

$(1\bar{1}0)_{Ti2ZrO}$, meanwhile those between the α-Ti and the spherical hexagonal Ti₂ZrO were $[0001]_{α\text{-}Ti}$ // $[0001]_{Ti2ZrO}$ and $(10\bar{1}0)_{α\text{-}Ti}$ // $(10\bar{1}0)_{Ti2ZrO}$.

References

1. R. L. Saha and K. T. Jacob, "Casting of Titanium and It's Alloy, " *Def. Sci.*, **36** [2]**,** 121-41 (1986).

2. R. Ruh, "Reaction of Zirconia and Titanium at Elevated Temperatures, " *J. Am. Ceram. Soc.*, **46** [7]**,** 301-06 (1963).

3. A. I. Kahveci and G. E. Welsch, "Effect of Oxygen on the Hardness and Alpha/Beta Phase Ration of Ti-6Al-4V Alloy, " *Scr. Metall.*, **20** [9]**,** 1287-90 (1986).

4. K. I. Suzuki, S. Watakabe, and K. Nishikawa, "Stability of Refractory Oxides for Mold Material of Ti-6Al-4V Alloy Precision Casting, " *J. Jpn. Inst. Met.*, **60** [8]**,** 734-43 (1996).

5. M. J. Donachie, *Titanium: A Technical Guide;* Ch. 11, p. 162, ASM International, Metals Park, OH, 1998.

6. G. Welsch and W. Bunk, "Deformation Modes of the Alpha-Phase of Ti-6AL-4V as a Function of Oxygen Concentration and Aging Temperature, " *Metall. Trans. A*, **13A** [5]**,** 889-99 (1982).

7. G. Economos and W. D. Kingery, "Metal-Ceramic Interactions: Ⅱ, Mteal Oxide Interfacial Reactions at Elevated Temperatures, " *J. Am. Ceram. Soc.,* **36** [12], 403-09 (1953).

8. R. Ruh, N. M. Tallan, and H. A. Lipsitt, "Effect of Metal Additions on the Microstructure of Zirconia, " *J. Am. Ceram. Soc.,* **47** [12], 632-35 (1964).

9. B. C. Weber, H. J. Garrett, F. A. Mauer, and M. A. Schwartz, "Observations on the Stabilization of Zirconia, " *J. Am. Ceram. Soc.,* **39**

[6], 197-07 (1956).

10. C. L. Lin, D. Gan, and P. Shen, "Stabilization of Zirconia Sintered with Titanium, " *J. Am. Ceram. Soc.,* **71** [8], 624-29 (1988).

11. R. F. Domagala, S. R. Lyon, and R. R., "The Pseudobinary Ti-ZrO2, " *J. Am. Ceram. Soc.,* **56** [11], 584-87 (1973).

12. C. F. Lin and C. C. Lin, "Transmission Electron Microscope Investigation of The Interface between Titanium and Zirconia, " *J. Am. Ceram. Soc.,* **82** [11], 3179-85 (1999).

13. G. Cliff and G. W. Lorimer, "The Quantitative Analysis of Thin Spectimens, " *J. Microsc.,* **130** [3], 203-07 (1975).

14. C. R. Brooks, *Heat Treatment, Structure and Properties of Nonferrous Alloys; C*h. 9, p. 329-87, American Society for Metals, Metals Park, OH, 1982.

15. L. A. Bendersky, A. Roytburd, and W. J. Boettinger, "Phase Transformations in The (Ti, Al)3Nb Section of The Ti-Al-Nb Systen-Ⅰ. Microstructural Predictions Based on A Subgroup Relation Between Phases, " A*cta Metall.,* **42** [7], 2323-335 (1994).

16. D. A. Porter and K. E. Easterling, P*hase Transformations in Metals and Alloys; Ch*. 5, p. 279, Chapman Hall, New York, 1992.

17. L. E. Fykin, V. V. Glazova, I. I. Kornilov, R. P. Ozerov, V. P. Smirnov, and S. P. Solov'ev, "Crystal Structure of the Suboxide Ti_2ZrO, " *Crystallography,* **13** [9], 845-48 (1969).

Table 2.1 Composition analysis of the starting material

Material	Composition(wt%)
Ti	0.25 O, 0.01 H, 0.03 N, 0.1 C, 0.3 Fe, 99.31 Ti
3Y-ZrO$_2$	> 94 ZrO$_2$+HfO$_2$*, 5.4 Y$_2$O$_3$, < 0.001 Fe$_2$O$_3$, < 0.01 SiO$_2$, < 0.005 Na$_2$O, < 0.005 TiO$_2$, < 0.02 Cl, < 0.005 SO$_4^{2-}$

*Accounts for approximately 2~3% of this total

Table 2.2 The calculated results of the hexagonal Ti$_2$ZrO structure factor

$h + 2k$	h and k	l	$\lvert F \rvert^2$
$3m, m = even$	even	even	$(f_{zr} + 2f_{Ti} + 3f_o)^2$
$3m, m = even$	even	odd	$(f_{zr} - 2f_{Ti} + 3f_o)^2$
$3m, m = even$	mixed	even	$(f_{zr} + 2f_{Ti} - f_o)^2$
$3m, m = even$	mixed	odd	$(f_{zr} - 2f_{Ti} - f_o)^2$
$3m, m = odd$	odd or mixed	even	$(f_{zr} + 2f_{Ti} - f_o)^2$
$3m, m = odd$	odd or mixed	odd	$(f_{zr} - 2f_{Ti} - f_o)^2$
$3m \pm 1, m = even$	odd or mixed	even	$(f_{zr} - f_{Ti} - f_o)^2$
$3m \pm 1, m = even$	odd or mixed	odd	$(f_{zr} + f_{Ti} - f_o)^2$
$3m \pm 1, m = odd$	mixed	even	$(f_{zr} - f_{Ti} - f_o)^2$
$3m \pm 1, m = odd$	mixed	odd	$(f_{zr} + f_{Ti} - f_o)^2$
$3m \pm 1, m = odd$	even	even	$(f_{zr} - f_{Ti} + 3f_o)^2$
$3m \pm 1, m = odd$	even	odd	$(f_{zr} + f_{Ti} + 3f_o)^2$

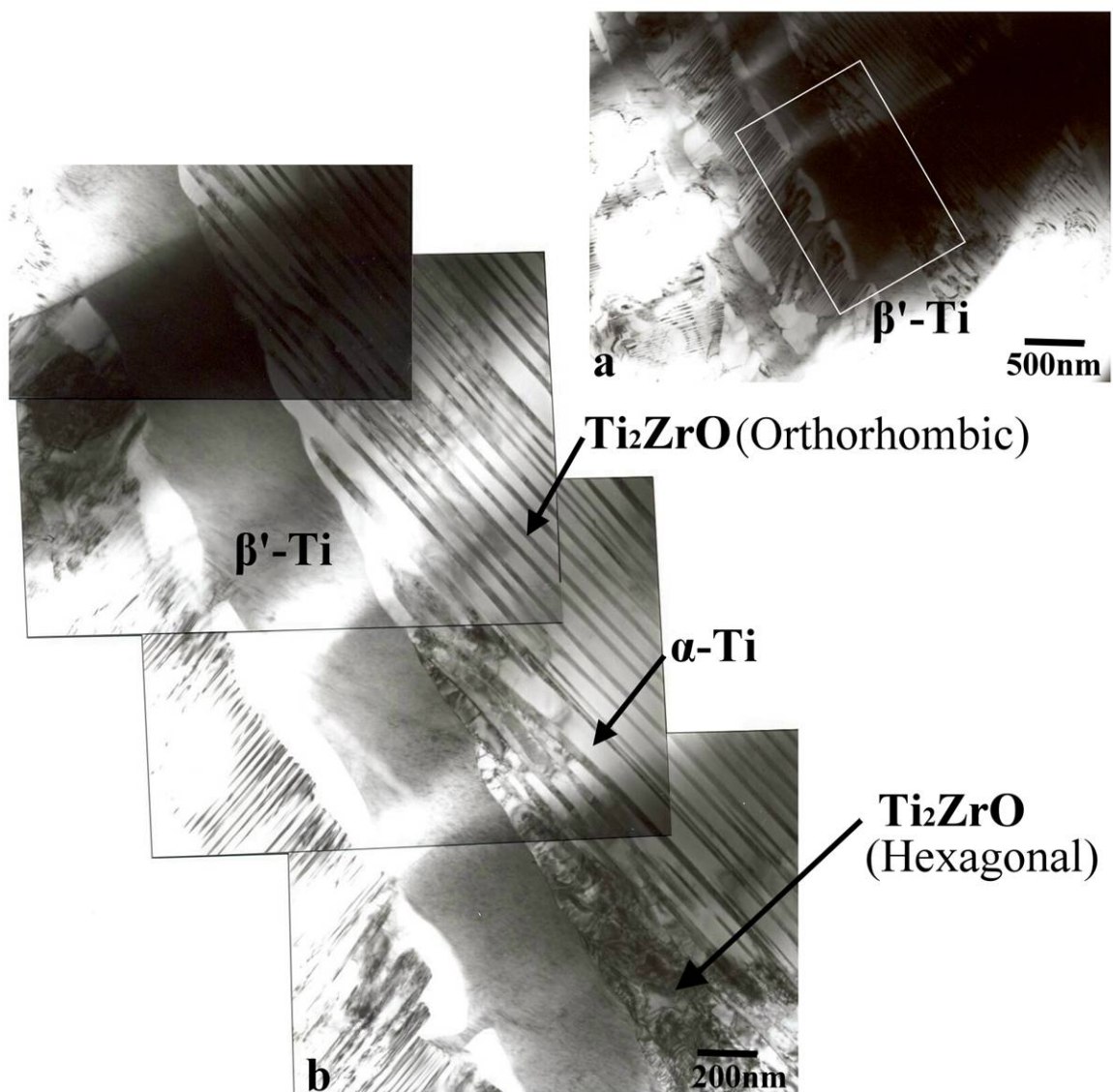* h, k, l and m are integer.

Fig. 2.1 (a) The TEM micrograph showing the interface between Cp-Ti and ZrO_2(3Y) after reaction at 1550℃/30min; (b) A magnified micrograph of the marked region in (a), indicating elongated β'-Ti and the lamellar structure of α-Ti and Ti_2ZrO in both sides of β'-Ti. The arrows in the lower right region indicate the spherical ordered Ti_2ZrO.
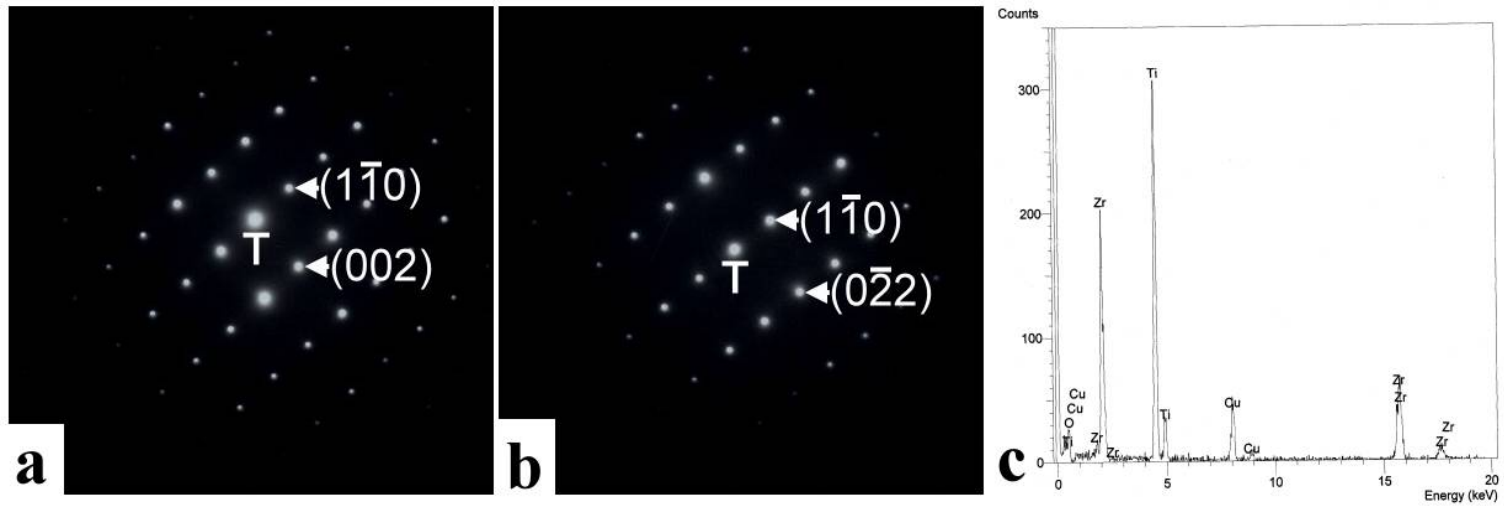
Fig. 2.2(a) and (b) SADP's of β'-Ti, Z=[110] $_{β'-Ti}$ and Z=[111] $_{β'-Ti}$, respectively ; (c) EDS of β'-Ti.

Fig. 2.3 (a) SADP's of the lamellar Ti$_2$ZrO and α-Ti, Z=[0001]$_{α\text{-}Ti}$ //[110]$_{Ti2ZrO}$; (b) EDS of α-Ti; (c) EDS of the lamellar Ti$_2$ZrO; (d) the standard stereographic projection with [0001]$_{α\text{-}Ti}$ //[110]$_{Ti2ZrO}$.
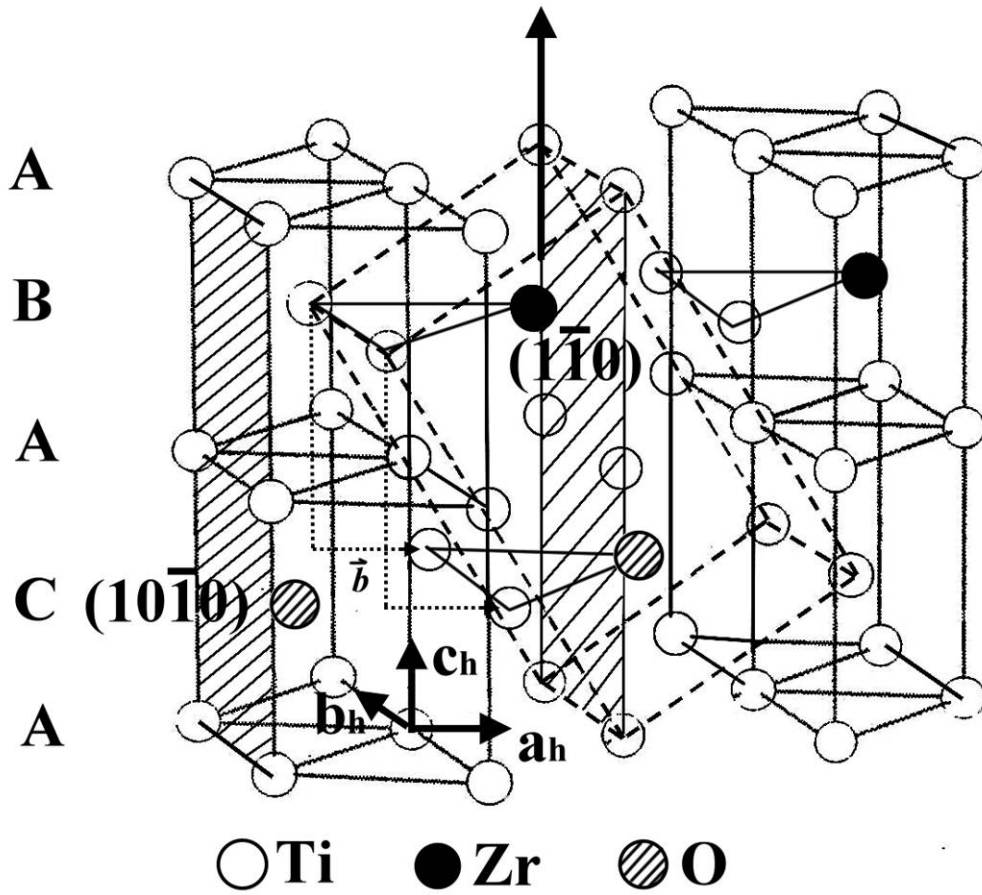
[0001]α-Ti//[110]Ti2ZrO

Fig. 2.4 The lattice relation of the orthorhombic Ti$_2$ZrO (dash line) and hexagonal α-Ti (soild line).
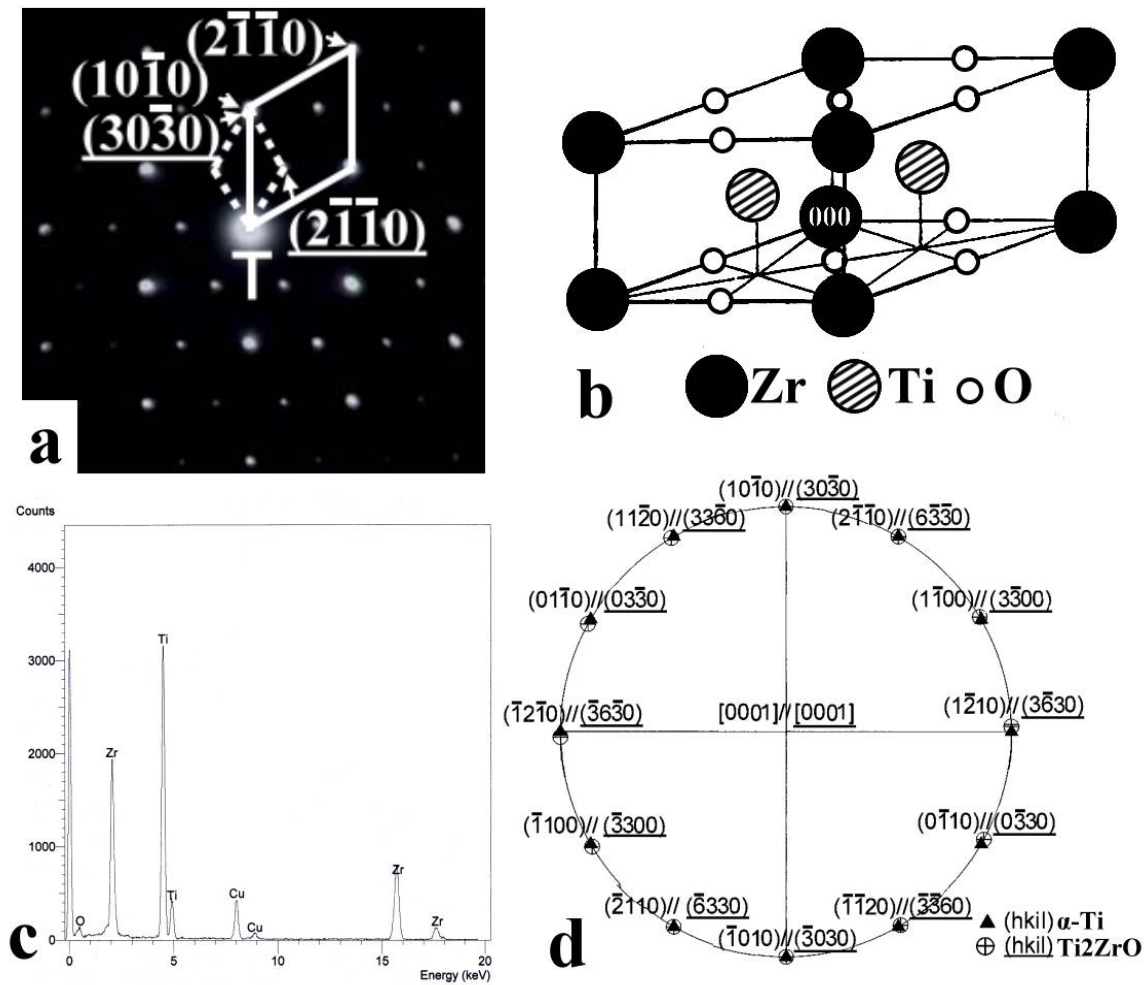
Fig. 2.5 (a) SADP's of the spherical ordered Ti$_2$ZrO and α-Ti, Z=[0001]$_{α\text{-}Ti}$ //[0001]$_{Ti2ZrO}$; (b) the hexagonal Ti$_2$ZrO unit cell [17]; (c) EDS of the spherical ordered Ti$_2$ZrO; (d) the standard stereographic projection with [0001]$_{α\text{-}Ti}$ //[0001]$_{Ti2ZrO}$.